SCIENCE CHINA
Chemistry

• ARTICLES •

April 2012 Vol.55 No.4: 632–642
doi: 10.1007/s11426-011-4482-9

Investigation of radionuclide ^{63}Ni(II) sequestration mechanisms on mordenite by batch and EXAFS spectroscopy study

YANG ShiTong, SHENG GuoDong, GUO ZhiQiang, TAN XiaoLi, XU JinZhang & WANG XiangKe*

Key Laboratory of Novel Thin Film Solar Cells, Institute of Plasma Physics, Chinese Academy of Sciences, Hefei 230031, China

Received October 27, 2011; accepted November 29, 2011; published online December 30, 2011

The sorption behavior and microscopic sequestration mechanisms of radionuclide ^{63}Ni(II) on mordenite as a function of aging time, ionic strength, initial ^{63}Ni(II) concentrations, solid content and coexistent electrolyte ions were investigated by the combination of batch and EXAFS techniques. Macroscopic experiment results show that the sorption of ^{63}Ni(II) is dependent on ionic strength at pH<7, and independent of ionic strength at pH>7. The sorption percentage of ^{63}Ni(II) on mordenite increases with increasing solid content, while the sorption capacity decreases as solid content increases. The presence of different electrolyte ions can enhance or inhibit the sorption of Ni(II) on mordenite in various degrees. EXAFS analysis results of the samples under three different ionic strengths suggest that the retained ^{63}Ni(II) in these samples exists in an octahedral environment with six water ligands. In the initial period of rapid uptake, the sorption of ^{63}Ni(II) is dominated by the formation of inner-sphere surface complexes. As aging time increases, ^{63}Ni(II) sequestration behavior tends to be mainly controlled by the formation of Ni phyllosilicate co-precipitates and/or $Ni(OH)_2(s)$ precipitates. Results for the second shell fit of the sample prepared at an initial ^{63}Ni(II) concentration of 100 mg/L indicate the possible formation of Ni polynuclear surface complexes. Both the macroscopic sorption data and the molecular level evidence of ^{63}Ni(II) surface speciation at the mordenite/water interfaces should be factored into better predictions of the mobility and bioavailability of ^{63}Ni(II) in environment mediums.

mordenite, ^{63}Ni(II), aging time, initial concentration, EXAFS analysis

1 Introduction

Along with the strategic requirements of environmental protection and global sustainable development, the promotion of economic and effective treatment methods for polluted aquatic environment to meet the increasingly stringent environmental standards has become a challenging job in environmental science and technology field. Various processing methods have been utilized for the disposal of heavy metals and radionuclides from aqueous solutions, such as physicochemical precipitation, ion exchange, ultrafiltration, reverse osmosis, electrodialysis, etc. Most of the processes have significant disadvantages such as high fussy operation, operational costs, secondary pollution, etc. In comparison, sorption has been identified to be superior to other techniques for wastewater purification due to its simplicity of design, convenience, low cost, high sorption efficiency and wide adaptability. Activated carbon, having strong sorption efficiency for various contaminants, is widely used as a good sorbent for the disposal of polluted waters [1–3]. However, it is beset with problems related to cyclic regeneration and contaminant recovery. In recent years, intensive research has focused on the seeking of low-cost materials with good metal-binding capacities, which can be utilized as an alternative to activated carbon in wastewater treatment.

Zeolites are microporous aluminosilicate minerals with well-defined structures, containing exchangeable alkaline

*Corresponding author (email: xkwang@ipp.ac.cn)

and alkaline earth metal ions (normally Na^+, K^+, Mg^{2+} and Ca^{2+}) as well as water in their structural framework. Many kinds of zeolites occur naturally as minerals, and are widespreadly distributed all over the world. Due to their outstanding properties such as featuring thermal stability, nanosized pore structures, and unusual surface topology, zeolites are widely used as promising support materials in the fields of catalytic industry, soil amendment, environmental protection and material science, etc. Recently, research has been focused on the utilization of zeolites in the decontamination of pollutants-laden wastewaters and various experimental results have been reported [4–6]. To predict the mobility and long-term behavior of heavy metal ions and radionuclides in environmental mediums, it is of fundamental importance to obtain a comprehensive understanding on their chemical speciation and sequestration mechanisms at zeolite/water interfaces.

In our previous study [7], we investigated the sorption mechanisms of Ni(II) on mordenite affected by solution pH, temperature and humic substances with the combination of batch and EXAFS techniques. The results suggested that the species of Ni(II) on mordenite changed from outer-sphere surface complexes to inner-sphere surface complexes and precipitates/co-precipitates with increasing pH values, and ternary surface complexes formed at HA/FA-mordenite hybrid surfaces. However, no valid data are available to expound the influence mechanism of aging time and ionic strength on the sorption and immobilization of Ni(II) on mordenite surfaces. In view of this point, further studies are needed to get more in-depth information that would be valuable for predicting the physicochemical behaviors of Ni(II) in environmental mediums. Herein we have expanded the study of Ni(II) sorption mechanisms on mordenite surfaces to distinguish the possible changes in interaction mechanisms. The effect of various environmental parameters such as aging time, ionic strength, solid content, initial Ni(II) concentrations and coexistent electrolyte ions on Ni(II) sorption behaviors in mordenite suspensions was investigated by using batch technique under ambient conditions. Specially, the speciation and local atomic structures of adsorbed Ni(II) on mordenite were investigated by using Ni K-edge EXAFS spectra to determine the influence of aging time, ionic strengths and initial Ni(II) concentrations on sorption mechanisms.

2 Materials and methods

2.1 Materials

The mordenite sample used here is the same as that applied in our previous study [7]. Inductively coupled plasma-atomic emission spectrometry (ICP-AES) analysis showed that the Si:Al radio in this mordenite sample is ca. 20:1. The cation exchange capacity (CEC) was determined to be 91 mmol/100 g by using ammonium acetate method. Besides, the zero point of charge (pH_{zpc}) of mordenite was measured to be ~4.5 by potentiometric titration procedure described in previous literature [8]. Radiotracer ^{63}Ni-NiCl was achieved from China Isotope Corporation with the radioactive chemistry concentration of 7.4×10^9 Bq/L. All the other chemicals were purchased in analytical purity and used without any further purification. Milli-Q water was used to prepare all the solutions.

2.2 Macroscopic experimental procedure

The macroscopic experiments were carried out in polyethylene tubes under ambient conditions by using batch technique. The stock suspension of mordenite and electrolyte solution were pre-equilibrated for 24 h and then Ni(II) stock solution including trace quantities of radiotracer ^{63}Ni-NiCl was added to achieve the desired concentrations of individual components. The solution pH was adjusted to the desired value with negligible amounts of 0.01 or 0.1 mol/L $HClO_4$ or NaOH. The suspensions were gently shaken for 2 d to attain sorption equilibrium, and then the solid was separated from solution by centrifugation at 14000 r/min for 30 min. The ^{63}Ni-NiCl concentration in supernatant was analyzed by liquid scintillation counting (Packard 3100 TR/AB Liquid Scintillation analyzer, PerkinElmer) with ULTIMA GOLD AB^{TM} (Packard) Scintillation cocktail. Under the assumption that the added radiotracer ^{63}Ni-NiCl dispersed evenly in the non-radioactive Ni(II) stock solution and both of them have similar sorption behaviors on mordenite, the sorption percentage of Ni(II) on mordenite was calculated from the initial activity of ^{63}Ni-NiCl (A_{tot}) in Ni(II) stock solution and that in supernatant (A_L) (i.e., $R\% = 100\% \times (1-A_L/A_{tot})$). All experimental data were the average of triplicate determinations and the relative errors were ~5%.

2.3 EXAFS analysis

2.3.1 Sample preparation for EXAFS analysis

Ni(II) sorption samples for EXAFS analysis were prepared by using a 250 mL vessel under various solution conditions. The sorption of Ni(II) was performed by adding 42.50 mL acidified 0.001 mol/L $Ni(ClO_4)_2$ stock solution and appropriate 0.1 mol/L NaOH to neutralize the acidity of this Ni(II) solution. The specific procedure was as follows: 10–50 μL increments of Ni(II) stock solution were added into the suspension under continuous stir to disperse the small aliquot of Ni(II) solution, and then base solution was added. Meanwhile, the solution pH was monitored and retained to the desired value during Ni(II) addition. Periods of a few minutes between the increments were selected to avert Ni(II)(aq) values exceeding the solubility limit of $Ni(OH)_2$(s), while allowing the accomplishment of Ni(II) addition in reasonable delay. After the desired aging time, aliquots of the suspension were collected and immediately centrifuged at 14000 r/min and 2 °C. The wet-paste was

then packed in a Teflon sample holder and covered with Mylar tape. The sample was wrapped in a moist paper towel and sealed in a Ziplock bag before it was removed from the glove box and transferred to the beam-line. XAFS data collection began less than 1 h after centrifugation.

2.3.2 *EXAFS analysis*

Ni K-edge X-ray absorption spectra at 8333 eV were recorded at the National Synchrotron Radiation Laboratory (NSRL, Hefei, China) in fluorescence mode. The electron storage ring was operated at 0.8 GeV with a maximum beam current of 200 mA. A superconductor wiggler with a maximum magnetic field B_0 of 6 T inserted in the straight section of the storage ring was used. The energy of X-ray was detuned by using a fixed-exit double-crystal Si (111) monochromator. Higher order harmonics were suppressed by detuning the monochromator by 25%. The monochromator position was calibrated by assigning the first inflection point on the K-absorption edge of metallic nickel foil to 8333.0 eV. Fluorescence spectra were collected using a multi-element pixel high purity Ge solid-state detector. Several scans were collected to improve the signal-to-noise ratio. Energy calibration and the EXAFS data analysis were performed with Athena and Artemis software interface to the IFEFFIT package [9]. The theoretical scattering phases and amplitudes used in data analysis were calculated by scattering code FEFF7 using the crystal structures of Ni(II)(aq), β-$Ni(OH)_2$(s) and $Ni_3Al_2SiO_8$ [10]. Accuracies for interatomic distance (R) and coordination number (CN) are 0.02 Å and 20%, respectively, for the first shell and 0.04 Å and 40%, respectively, for the second shells.

3 Results and discussion

3.1 Macroscopic experiment results

3.1.1 *Effect of aging time*

Figure 1 shows the sorption of Ni(II) on mordenite as a function of aging time at pH 7.2. One can see that the kinetics process of Ni(II) on mordenite was initially fast, with 38% uptake occurring in the first 30 min. Subsequent uptake continued slowly and about 72% was adsorbed after 60 d of aging time. Changes in uptake were insignificant after 15 d. The high initial uptake rate may be attributed to the existence of plentiful sorption sites on mordenite surfaces. As the sites being gradually filled up, the sorption becomes slow and the mechanism of kinetics seems to be more dependent on various factors such as sorption to less reactive sites, diffusion to internal sites, surface substitution, and formation of multinuclear complexes and/or surface precipitates [11–14]. In the following experiments, the aging time was restricted to 2 d to avoid the formation of multinuclear complexes or surface precipitates.

3.1.2 *Effect of ionic strength*

The ionic strength has a great impact on the migration and transformation of metal ions in environmental medium, which will further influence the purification processes of water pollutants. Evaluation of ionic strength effect on sorption behavior is an effective macroscopic method of inferring sorption mechanisms. As is well-known, ClO_4^- does not form complexes with the concomitant metal ions in solution. In view of the above reasons, to help compare and analyze the role of ionic strength variation, experiments are conducted to determine the sorption of Ni(II) on mordenite in 0.001, 0.01 and 0.1 mol/L $NaClO_4$ electrolyte solutions despite the fact that ClO_4^- is not the common ion in aqueous environment. One can see from Figure 2 that the sorption percentage of Ni(II) on mordenite is strongly affected by ionic strength at pH<7 and no obvious effect is found at pH>7. From the ionic strength dependence, one can deduce that cation exchange of Ni^{2+} (the dominant Ni(II) species at low pH) with Na^+/Ca^{2+} that saturates the exchangeable sites is the main mechanism for Ni(II) sorption on mordenite at pH<7 [15, 16], which is also supported by the very slow increase of Ni(II) sorption at this pH range. The phenome-

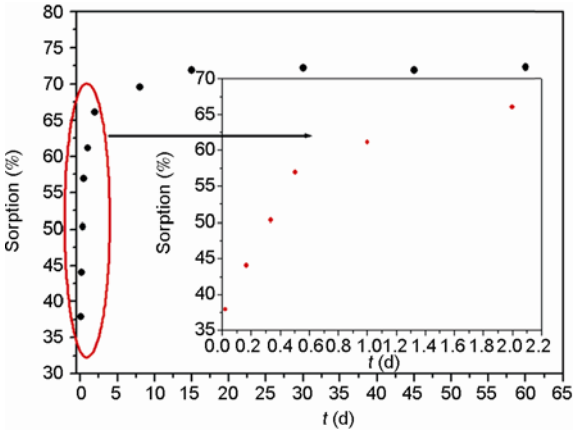

Figure 1 Effect of aging time on Ni(II) sorption on mordenite. T = 293 K, m/V = 0.5 g/L, $C_{Ni(II)initial}$ = 10 mg/L, I = 0.01 M $NaClO_4$.

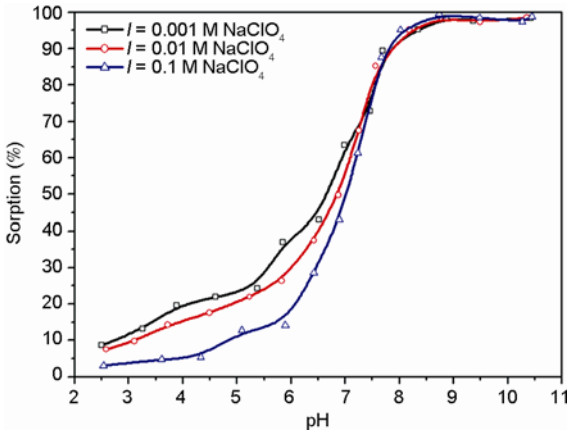

Figure 2 Effect of ionic strength on Ni(II) sorption on mordenite. T = 293 K, m/V = 0.5 g/L, $C_{Ni(II)initial}$ = 10 mg/L [7].

non that Ni(II) sorption is not influenced by the variance of ionic strength at pH>7 is compatible with the formation of inner-sphere complexes. The activity coefficients of Ni(II) ions in 0.001, 0.01 and 0.1 mol/L $NaClO_4$ electrolyte solution are 0.870, 0.675 and 0.405 [17], respectively. On the basis of this value, one can deduce that the actual chemical activity values for an initial Ni(II) concentrations of 10 mg/L in 0.001, 0.01 and 0.1 mol/L $NaClO_4$ electrolyte solutions are 8.70, 6.75 and 4.05 mg/L, respectively. Based on the solubility product constant of $Ni(OH)_2(s)$ (K_{sp} = 2.0 × 10^{-15}) [17], it is calculated that Ni(II) ions begin to form hydroxide precipitates at pH 8.5, 8.6 and 8.8 for an actual Ni(II) chemical activity of 8.70, 6.75 and 4.05 mg/L, respectively. Correspondingly, it is clear that the sorption process of Ni(II) on mordenite under high alkaline conditions (herein, pH>8.5) are mainly attributed to the formation of hydroxide precipitates.

As can be seen from Figure 2, the sorption of Ni(II) on mordenite increases with decreasing ionic strength at pH<7, which is consistent with increased sorption on the permanent charge sites with decreasing Na^+ concentration. This phenomenon may derive from the following reasons: (1) As mentioned above, increased ionic strength decreases the activity of Ni(II) ions in solution, which correspondingly limits their transfer to mordenite surfaces [18, 19]; (2) ionic strength can affect particle aggregation by influencing electrostatic interactions. Increased ionic strength can reduce electrostatic repulsion and thereby increase particle aggregation of mordenite, which reduces the amount of available binding sites and thereby decreases the sorption of Ni(II) on mordenite [20]; (3) the thickness of electrical diffused double layer surrounding mordenite particles and Ni(II) ions can be significantly expanded by the presence of electrolyte ions. Such expansion prevents mordenite particles and Ni(II) ions from approaching each other more closely and accordingly leading to the decrease of Ni(II) sorption via the lessening of electrostatic attraction [21].

3.1.3 *Effect of initial Ni(II) concentrations*

Figure 3 shows Ni(II) sorption on mordenite at three differ-ent initial Ni(II) concentrations as a function of pH values. The sorption curves show a typical "sorption edge", namely, the sorption percentage practically increases from zero to ~99% over a range of more than three pH units. As expected, the pH-edge shifts to higher pH values at higher Ni(II) concentration. In a pH region below approximate pH 8.0, the sorption percentage of Ni(II) increases with decreasing initial Ni(II) concentration. On the other hand, in the pH region where the sorption percentage of Ni(II) increases sharply up to ~99%, the sorption data exhibit no dependence on initial Ni(II) concentrations. It is necessary to determine whether the formation of $Ni(OH)_2(s)$ precipitates contributes to the rapid increase of Ni(II) sorption on mordenite at pH<8.0. Once again, based on the activity coefficient value of Ni(II) in 0.01 mol/L $NaClO_4$ solution (i.e., 0.675), the actual chemical activity values for an initial Ni(II) concentrations of 5, 10 and 100 mg/L are calculated to be 3.375, 6.75 and 67.5 mg/L, respectively. Considering the solubility product constant of $Ni(OH)_2(s)$ (K_{sp} = 2.0 × 10^{-15}) [17], one can deduce that Ni(II) ions begin to form hydroxide precipitates at pH 8.8, 8.6 and 8.1 for an actual Ni(II) chemical activity of 3.375, 6.75 and 67.5 mg/L (corresponding initial Ni(II) concentrations are 5, 10 and 100 mg/L), respectively. However, it is clear that more than 90% Ni(II) is adsorbed on mordenite at pH 8.0. Hence, the draft increase of Ni(II) sorption on mordenite at pH<8.0 is not attributed to the surface precipitation of $Ni(OH)_2(s)$. The actual mechanism that accounts for the observed sorption trend will be discussed in detail in the following EXAFS analysis section.

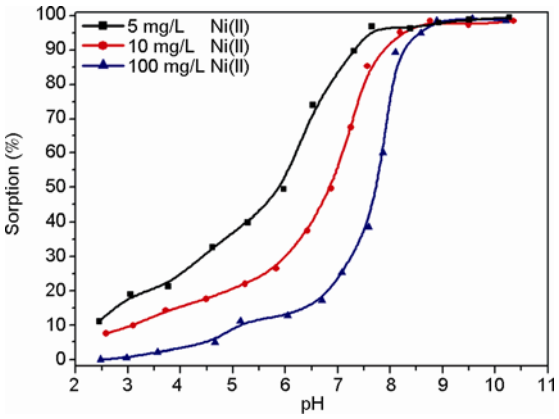

Figure 3 Sorption of Ni(II) on mordenite as a function of initial concentrations. T = 293 K, m/V = 0.5 g/L, I = 0.01 M $NaClO_4$.

3.1.4 *Effect of solid content*

The sorption of Ni(II) on mordenite at different solid content was studied at T = 293 K and pH 7.2. As can be seen from Figure 4, the sorption percentage of Ni(II) increases rapidly with increasing solid content at m/V<1.0 g/L, and then maintains unchanged with the increase of solid content

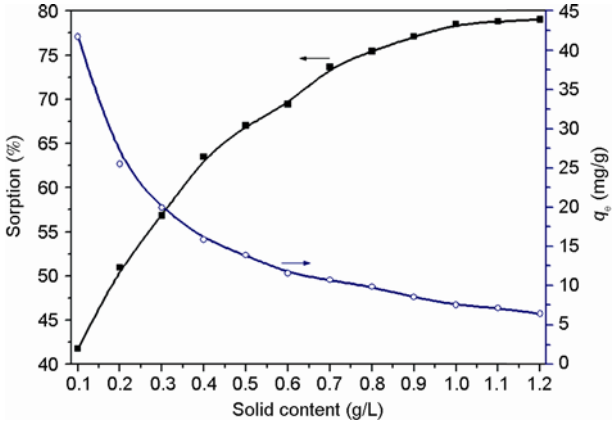

Figure 4 Sorption of Ni(II) on mordenite as a function of solid content. T = 293 K, pH 7.2, $C_{Ni(II)initial}$ = 10 mg/L, I = 0.01 M $NaClO_4$.

at m/V>1.0 g/L. With increasing solid content, the number of functional groups on mordenite surfaces increases and thereby more surface sites are available for binding Ni(II).

One can also see from Figure 4 that the sorption capacity of Ni(II) on mordenite decreases gradually with the increase of solid content. The mordenite surface is composed of sites with a spectrum of binding energies. At low solid content, all types of surface sites are entirely exposed for sorption and the surface reaches saturation quickly, leading to a higher sorption capacity. But at higher solid content the availability of higher energy sites decreases with a larger fraction of lower energy sites becoming occupied, resulting in a lower sorption capacity [22]. Besides, higher solid content increases the probability of particle collision and therefore creates the aggregation of mordenite particles, resulting in a decrease in the total surface area and an increase in diffusional path length, both of which lead to the decrease of sorption capacity [23]. Another possible interpretation is that the increase ratio of net sorption quantity of Ni(II) on mordenite surface is lower than that of solid content, which correspondingly decreases the sorption capacity of Ni(II) on mordenite.

3.1.5 *Effects of coexistent electrolyte ions*

Figure 5 shows the sorption of Ni(II) on mordenite as affected by common electrolyte ions in solution, viz., ClO_4^-, NO_3^-, Cl^-, SO_4^{2-}, Li^+, Na^+, K^+ and Ca^{2+}, respectively. Except for Li^+, NO_3^- and ClO_4^-, all the other ions are among the most common inorganic electrolyte ions in natural water systems. Although Li^+ and NO_3^- are not present in natural water bodies, their concentrations in contaminated water can not be ignored due to their widespread applications in industrial and agricultural production processes. Hence, it is necessary to determine the effects of these two ions on the physicochemical behaviors of heavy metal ions and radionuclides in environmental mediums. As mentioned above, complexation can not occur between ClO_4^- and the coexisting metal ions in solution. In view of this point, to help discriminate and analyze the role of various electrolyte cations, related experiments were processed in $MClO_4$ (M represents cations) electrolyte solutions despite the fact that ClO_4^- is not the common ion in aqueous environment. Similarly, the batch experiments for comparing the influence of electrolyte anions were conducted in NaX (X represents anions) solutions.

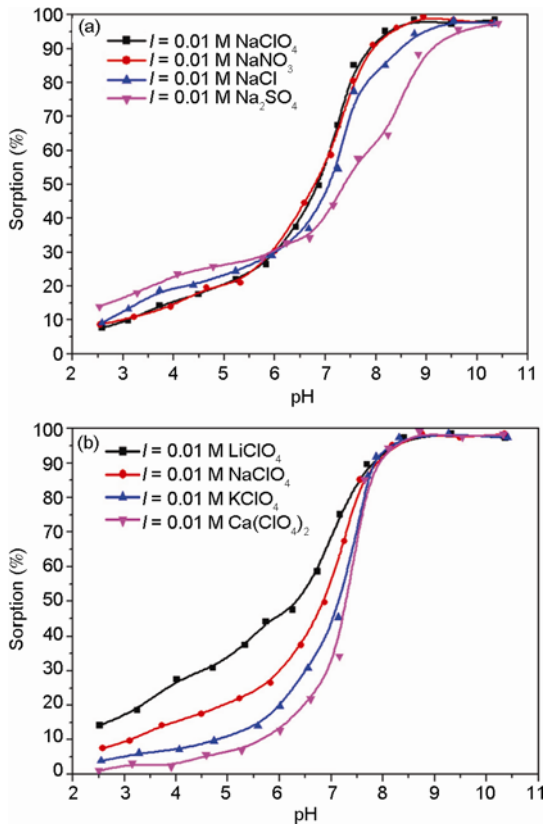

Figure 5 Influence of coexistent electrolyte anions (a) and cations (b) on the Ni(II) sorption on mordenite. T = 293 K, $C_{Ni(II)initial}$ = 10 mg/L, m/V = 0.5 g/L.

From Figure 5(a), one can see that the sorption of Ni(II) on mordenite is greatly influenced by electrolyte anions in solution. Taking the sorption of Ni(II) in ClO_4^- electrolyte solution as a point of reference, it is clear that NO_3^- has little influence on Ni(II) sorption. The presence of Cl^- and SO_4^{2-} enhances Ni(II) sorption at pH<5.5, while reduces Ni(II) sorption at pH>5.5. The result is not in accordance with that of Eu(III) sorption on titanate nanotubes [24]. The nature of the counter-ions, destined to stabilize heavy metal ions in the cationic form, can also influence their sorption on solid particles. Briefly, electrolyte anions may either enhance or reduce metal ion sorption via site competition, surface charge alteration and the formation of solution complexes, ternary complexes and/or surface precipitates [25–27]. Specifically, the enhancement of Cl^- on Ni(II) uptake at pH<5.5 is to some extent attributed to the formation of complexes between Ni(II) ions and Cl^- (e.g., $NiCl^+$), which decreases the electropositivity of Ni(II) ions and thereby promotes the sorption of positively Ni(II) ions on mordenite due to the decrease of electrostatic repulsion. Enhanced affinity of $NiCl^+$ complex relative to the free Ni^{2+} ions for mordenite surfaces can reduce the electrostatic barrier that Ni(II) must overcome when adsorbed to the positive mordenite surfaces ($pH<pH_{zpc}$). In SO_4^{2-} electrolyte solution, the enhancement of Ni(II) sorption on mordenite at pH<5.5 may be attributed to the formation of ternary complexes. Besides, the idiocratic sorption of SO_4^{2-} on mordenite enhances the electronegativity of mordenite surface and thereby promotes the sorption of positively charged Ni(II) ions due to electrostatic attraction. At high pH values, Cl^- and SO_4^{2-} are difficult to be adsorbed on the negatively charged surfaces of mordenite due to electrostatic repulsion. The competition between Cl^-/SO_4^{2-} and mordenite increases the formation of Ni(II)-Cl^-/SO_4^{2} stable complexes in solution, which competitively diminishes the extent of Ni(II)

sorption on mordenite. From the above discussion, it is clear that the sorption of Ni(II) on mordenite is greatly dependent on the types electrolyte ions. However, the mechanism of specific electrolytes anions on Ni(II) sorption is difficult to be discriminated solely from the macroscopic experiment data and further investigation is needed to obtain in-depth microstructure information.

As can be seen from Figure 5(b), the four electrolyte cations exhibit distinct effect on Ni(II) sorption. The sorption of Ni(II) on mordenite at the same pH values is in the sequence of Ca^{2+}<K^+<Na^+<Li^+ at pH<7.5, while no obvious effect is found at high pH values. The hydration radius of K^+ (2.32 Å) is smaller than the radii of the Na^+ (2.76 Å) and Li^+ (3.40 Å) and accordingly the influence of K^+ on Ni(II) sorption is more obvious than that of Na^+ and Li^+ [28]. The result is consistent with that of Th(IV) sorption on TiO_2 [29]. It is worth noting that Ca^{2+} has a greater competition effect towards Ni(II) sorption than Li^+, Na^+ and K^+. Harter and Naidu claimed that the sorption percentage of cations decreased with the increasing valence of competitive cations because the increasing of cation valence made the surface potential less negative at pH values greater than pH_{zpc} [30]. The cations with higher valence are much easier to be adsorbed by mordenite, and the divalent cations would occupy twice sites more competitively by forming $(=SO)_2$–Ca. Accordingly, the influence of bivalent Ca^{2+} on Ni(II) sorption is stronger than monovalent Li^+, Na^+ and K^+.

The above-mentioned results show that the sorption of Ni(II) on mordenite is greatly influenced by coexistent electrolyte ions under our experimental conditions. However, the effect of electrolyte anions on Ni(II) sorption on Na-bentonite and Pb(II) sorption on oxidized MWCNTs was reported to be negligible [31, 32]. Besides, the effect of electrolyte cations on Ni(II) sorption on ACT-attapulgite is in the sequence of Li^+>Na^+>K^+ [33], which is opposite to the result in this study. Comparing the results in our experiment with those in the above-mentioned literature, one can draw a conclusion that the influence of coexistent electrolyte ions on metal ions' sorption is dominated by various factors such as the properties of metal ions, the properties of adsorbents, the affinities of electrolyte ions on the binding sites and other environmental parameters such as pH, ionic strength, etc. Therefore, it is necessary to improve the selective sorption property of the adsorbent for a given metal ion. One effective way to achieve selective sorption is to change the surface properties of mordenite by modifying its surface with specific chemicals. It is well known that the binding of cations to solid surfaces can be influenced by the chemical nature of binding sites (e.g. phenolic hydroxyl versus carboxylic) and by the spatial arrangement of the potential binding sites. For instance, some metal ions preferentially form complexes with O-containing functional groups, while others preferentially form complexes with S–, N–, or P–containing functional groups. In addition, carboxylic sites are more selective toward multivalent cations when the sites are attached to adjacent carbon atoms on a ring structure than when they are more widely spaced [34]. Based on these theories, selective sorption can be achieved by modifying mordenite surfaces with chemicals that possess desired functional groups.

3.2 EXAFS data analysis

The k^3-weighted EXAFS spectra of Ni(II) adsorbed on mordenite at different aging times are shown in Figure 6(a). One can see that the spectra appear distinct and differ from

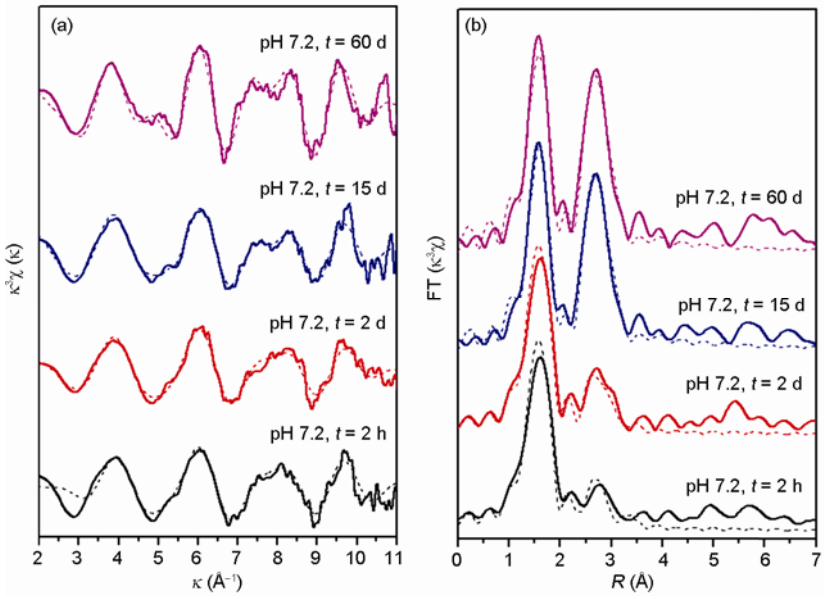

Figure 6 k^3-weighted spectra (a) and radial structure functions (RSFs) (b) produced by forward Fourier transforms (uncorrected for phase shift) of Ni(II) sorption on mordenite at various aging time. Solid and dash lines represent experimental spectra and spectral fits, respectively. m/V = 0.5 g/L, pH 7.2, T = 293 K, $C_{Ni(II)initial}$ = 10 mg/L, I = 0.01 mol/L $NaClO_4$.

either the reference samples (Ni(II)(aq) or β-$Ni(OH)_2$(s)) [7, 12, 35]. As aging time increases, more highly structured features appear and correspondingly change the shapes of EXAFS oscillations at k positions of ~5.0 and 7.5 $Å^{-1}$. The frequency components corresponding to these changes are probably attributed to the contribution of second neighbor atoms surrounding the central Ni atom. In order to isolate the characteristic frequencies that exist in the k^3-weighted EXAFS spectra, the EXAFS data are Fourier transformed to yield the corresponding radial structure functions (RSFs) and the results are shown in Figure 6(b). One can see that all the spectra show a main peak at 1.6 Å (phase shift uncorrected), which corresponds to the signal of oxygen atoms in the first coordination shell. Furthermore, the appearance of additional frequencies in the region between 2.3 and 3.4 Å is attributed to the higher coordination shells (i.e., Ni–Al, Ni–Si and/or Ni–Ni), which is suggestive of the formation of inner-sphere complexes, coprecipitates and/or hydroxide precipitates. For samples with aging time over 2 d, the intensity of the peak at ~2.8 Å (phase shift uncorrected) is considerably larger than that for the sample with aging time up to 2 d, which is indicative of increasing contribution from heavy backscattering atoms with increasing aging time.

Quantitative analysis results for the spectra fitting of the samples with different aging times are shown in Table 1. Structural parameters of the first coordination shell show that the central Ni atom is coordinated with ~6 O atoms with an average Ni–O interatomic distance ($R_{Ni–O}$) of ~2.04 Å for all samples, which reveal that there is no consistent change in first coordination shell environment with increasing aging time. Results for the second shell fit can be divided into two groups: one group includes samples with Ni–Al and Ni–Si backscatterings, and the other has samples with both Ni–Ni and Ni–Si backscatterings. For samples reacted up to 2 d, summary results (Table 1) indicate that the coordination numbers of second shell neighbors were 1.1–1.2 and 1.9–2.8 for Ni-Al and Ni-Si, respectively. The plausible models of Ni(II) surface complexes can be deduced by combining the quantitative results from EXAFS spectra analysis of sorption samples with the polyhedral structure of mordenite. The oxygen-oxygen (O–O) edge distances in $Ni(II)O_6$ octahedron are approximately 2.88 Å, while O–O edge distances of $Al(O,OH)_6$ octahedra and $Si(O,OH)_4$ tetrahedra in mordenite structure range from 2.69 to 2.90 Å and 2.56 to 2.67 Å, respectively [36, 37]. The similarity between the O–O edge distance in $Ni(II)O_6$ octahedron and that in $Al(O, OH)_6$ octahedron indicates that $Ni(II)O_6$ can bond to $Al(O,OH)_6$ octahedra in either corner-shared or edge-shared modes without much strain. In contrast, the significant difference between the O–O edge distance in $Ni(II)O_6$ octahedron and that in $Si(O,OH)_4$ tetrahedron should cause considerable strain if $Ni(II)O_6$ were to bond to $Si(O,OH)_4$ tetrahedron in edge-shared mode. Consequently, corner-shared bonding between $Ni(II)O_6$ and $Si(O,OH)_4$ tetrahedron should be more energetically favorable than edge-shared bonding. More specifically, the interatomic distances derived from the EXAFS spectra fitting are the characteristic of edge-shared linkage between $Ni(II)O_6$ octahedron and $Al(O,OH)_6$ octahedra, and of corner-shared linkage between $Ni(II)O_6$ octahedron and $Si(O,OH)_4$ tetrahedron [7, 38, 39]. In addition, the absence of Ni second neighbor atoms suggests that no Ni polynuclear surface complexes or surface precipitates formed at short aging time.

For samples with aging time up to 15 and 60 d, the best fits for the filtered second shell of the EXAFS spectra are obtained by using Ni–Ni and Ni–Si backscattering paths. As mentioned above, the period of slow uptake may be attributed to diffusion to internal sites, surface substitution, surface polymerization and/or the formation of precipitates/co-precipitates [11–14, 40, 41]. In case of surface substitution, the coordination number of neighboring atoms and interatomic distances between the metal center and neigh-

Table 1 Structural parameters derived from EXAFS analysis for Ni sorption samples

Sample conditions	First shell (Ni–O)			Second shell (Ni–Ni/Al/Si)				% Res
	R (Å)	CN	σ^2 (Å^2)	bond	R (Å)	CN	σ^2 (Å^2)	
pH 7.2, 10 mg/L Ni(II), 2 h	2.05	5.7	0.005	Ni–Al	3.02	1.1	0.007	9.7
				Ni–Si	3.28	1.9	0.007	
pH 7.2, 10 mg/L Ni(II), 2 d	2.03	5.9	0.003	Ni–Al	3.00	1.2	0.007	11.2
				Ni–Si	3.27	2.8	0.007	
pH 7.2, 10 mg/L Ni(II), 15 d	2.04	6.1	0.004	Ni–Ni	3.07	2.9	0.007	10.2
				Ni–Si	3.28	3.4	0.007	
pH 7.2, 10 mg/L Ni(II), 60 d	2.04	5.8	0.003	Ni–Ni	3.08	3.2	0.007	9.9
				Ni–Si	3.27	4.1	0.007	
pH 6.5, 10 mg/L Ni(II), I = 0.001 M	2.05	6.1	0.003					6.2
pH 6.5, 10 mg/L Ni(II), I = 0.01 M	2.04	5.9	0.003					7.9
pH 6.5, 10 mg/L Ni(II), I = 0.1 M	2.03	5.6	0.004					9.5
pH 7.2, 100 mg/L Ni(II)	2.03	5.8	0.003	Ni–Ni	2.95	1.8	0.007	10.2

R, Interatomic distance; CN, coordination number; σ^2, Debye-Waller factor; Res, a measure of the agreement between experimental and theoretical EXAFS curves.

boring atoms should be consistent with the structure of the solid phase [42]. However, the average R_{Ni-O} value for the long-time samples (~2.04 Å) does not match the average R_{Al-O} value for $Al(O,OH)_6$ octahedron (1.85–1.97 Å) and R_{Si-O} value for $Si(O,OH)_4$ tetrahedra (1.56–1.64 Å) in mordenite structure [36, 37]. The great dissimilarities in the cation-oxygen distances and the coordination numbers suggests that surface substitution of Ni for Al/Si structural sites is not the driving force for Ni(II) sorption on mordenite surfaces. One can see from Table 1 that the central Ni is surrounded by 2.9–3.2 Ni at Ni–Ni interatomic distance of ~3.07 Å and 3.4–4.1 Si at Ni–Si interatomic distance of ~3.28 Å, suggesting the formation of mixed Ni–Si surface coprecipitate (i.e., Ni phyllosilicate) [43, 44]. However, it is worthy pointing out that Ni hydroxide precipitates can not be excluded due to the similarity of EXAFS spectra for $Ni(OH)_2$(s) and Ni phyllosilicate with the sorption samples [12], and thus a mixture of $Ni(OH)_2$(s) precipitates and Ni phyllosilicate formed after the aging time of 15 d. The relative contribution of these two products to the overall Ni(II) uptake needs further investigation. The time-variant nature of Ni(II) sorption on mordenite is in accordance with earlier reports in which continued Ni(II) uptake was attributed to the formation of surface-induced Ni (co)precipitates [45–47]. However, Strathmann *et al*. postulated that the time-invariant nature of Ni(II) sorption on boehmite at low concentration was attributed to the formation of inner-sphere complexes [48]. The differences between the results in this work and the above-mentioned literature are mainly attributed to the distinct surface properties of applied materials.

The k^3-weighted EXAFS spectra and the corresponding Fourier transformed RSFs for the sorption samples prepared at different ionic strengths are shown in Figure 7. The k^3-weighted spectra (Figure 7(a)) are dominated by a single sinusoid and the spectral noise is more pronounced at high ionic strength due to the low Ni loading on the surface. There is a large decrease in the amplitude of the signal at k>10 Å^{-1} as a result of dampening of the EXAFS signal due to a large amount of structure disorder and thermal disorder as well as the lack of high shell back-scattering in the local atomic structure of the central Ni atom. The corresponding RSFs of these samples (Figure 7(b)) show only a single peak at ~1.6 Å (phase shift uncorrected), indicating a single shell of back-scattering O atoms was located neighboring the central Ni atom. The lack of a second peak in the RSFs is consistent with the formation of hydrated outer-sphere complexes on the permanent charge layer of mordenite. Fitting results of the first shell (Ni–O) show that Ni was coordinated with ~6 O atoms at an interatomic distance of 2.03–2.05 Å for all samples (Table 1). Although there is a small decrease in distance with increased ionic strength, these bond distances suggest that there is no substantial change in the first shell coordination environment due to ionic strength changing. The interatomic distances and coordination numbers indicate that the retained Ni(II) in these samples exists in an octahedral environment with six water ligands. The results imply that Ni(II) is retained via the cation exchange process between Ni^{2+} and Na^+/Ca^{2+} that saturate the exchangeable sites or electrostatic sorption in a diffuse layer swarm. However, EXAFS technique is not able to discriminate these two modes because the second shell structural atoms are too distant to be detected.

For the sample prepared at initial Ni(II) concentration of 100 mg/L, pronounced features appear in the higher k positions at ~5 Å^{-1} and ~8 Å^{-1} (Figure 7(a)), implying the

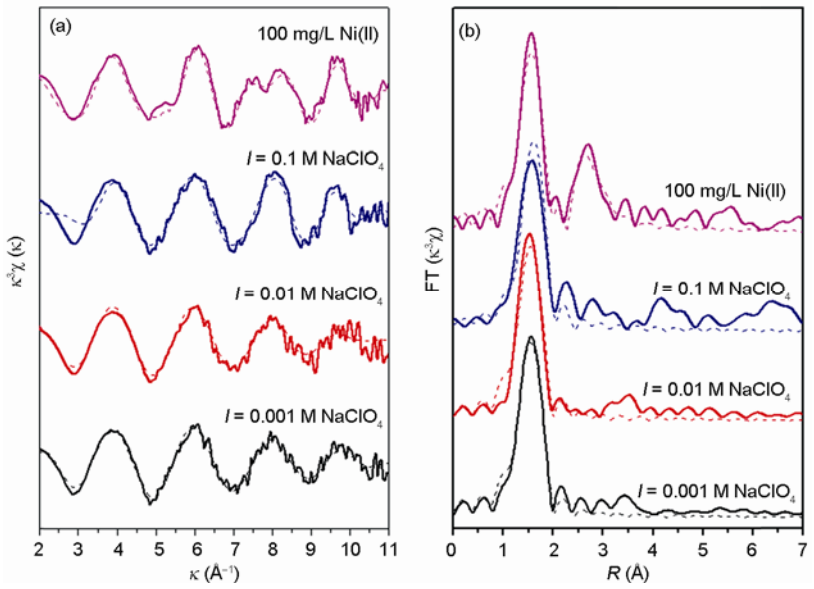

Figure 7 k^3-weighted spectra (a) and radial structure functions (RSFs) (b) produced by forward Fourier transforms (uncorrected for phase shift) of Ni(II) sorption on mordenite as a function of ionic strength and initial concentrations. Solid and dash lines represent experimental spectra and spectral fits, respectively. m/V = 0.5 g/L, T = 293 K.

presence of heavy back-scattering atoms in the local coordination environment of retained Ni [38, 39, 46]. In the corresponding RSF (Figure 7(B)), a further peak with intensity evidently above the background is present between 2.3 and 3.4 Å, suggesting the presence of structure beyond the first coordination shell. These features indicate the presence of more than one ordered neighboring shell around Ni atoms, and therefore the outer-sphere surface complexation is not the predominant sorption mode under this condition. Results for the second shell fit show only Ni–Ni backscattering at the interatomic distance of 2.95 Å with the coordination number of 1.8 (Table 1). The presence of Ni second neighbor atoms indicates the possible formation of Ni polynuclear surface complexes or surface precipitates. The shorter distance of the Ni–Ni bond in the phase (2.95 Å) relative to that of $Ni(OH)_2$(s) (~3.10 Å) [7, 12, 35] suggests that the structure of this sample is not crystalline hydroxide precipitates but a modified form appropriate to the mordenite structure. Attempts to include Al/Si atoms with Ni atoms in the second shell fitting were not successful due to improbable fitting parameters with low accuracies (data not shown). The absence of Al/Si contributions in the second shell indicates that the formation of mixed metal surface precipitates did not occur for samples at the initial Ni(II) concentration of 100 mg/L. Alternatively, the lack of Al/Si second neighbor backscattering could be attributed to the amplitude cancellation effect of Al/Si and Ni, where the weak amplitude of a light element such as Al and Si could be canceled by the overlapping of heavier Ni–Ni backscattering [41, 49]. Furthermore, the sensitivity of the EXAFS signal for weak second-shell backscattering atoms such as Al/Si is low and the small coordination number of these elements is difficult to recognize, leading to the absence of Al/Si in the second shell fitting.

4 Potential sequestration mechanisms

Macroscopic and spectroscopic techniques were combined to determine the sorption behavior and sequestration mechanisms of radionuclide ^{63}Ni(II) on mordenite. Macroscopic experiment results show that the sorption of Ni(II) is dependent on ionic strength at low pH values, and independent of ionic strength at high pH values. The presence of different electrolyte ions can enhance or inhibit the sorption of Ni(II) on mordenite in various degrees. The various results are attributed to the different complexing abilities of these electrolyte ions with Ni(II) ions and the difference in their affinities on the binding sites of mordenite. EXAFS analysis results of the samples at different ionic strengths suggest that Ni(II) is retained via the ion exchange process, leading to the formation of outer-sphere complexes (Figure 8(a)). The quantitative analysis results of EXAFS spectra indicate that the kinetics of Ni(II) sorption on mordenite surfaces can be assigned to two distinct mechanisms. In the initial period of rapid uptake, the sorption of Ni(II) is dominated by the formation of inner-sphere surface complexes (Figure 8(b)). As aging time increases, the formation of Ni phyllosilicate

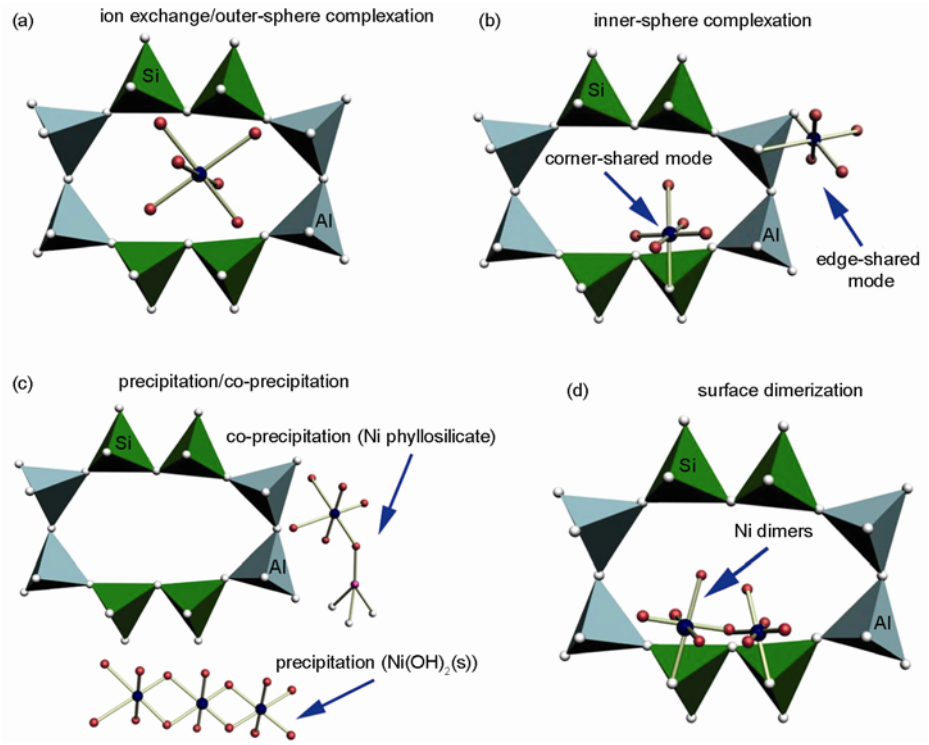

Figure 8 Schematic presentation of the possible mechanisms of Ni(II) sequestration on mordenite surfaces: (a) Ion exchange/Outer-sphere surface complexation; (b) inner-sphere surface complexation; (c) precipitation/co-precipitation; (d) surface dimerization.

co-precipitates and/or $Ni(OH)_2(s)$ precipitates tends to be the main driving force for Ni(II) sequestration under our experimental conditions (Figure 8(C)). Results for the second shell fit of the sample prepared at an initial Ni(II) concentration of 100 mg/L indicate the possible formation of Ni polynuclear surface complexes (e.g., binuclear dimers) (Figure 8(D)).

The sequestration of Ni(II) ions on mordenite surfaces has a significant influence on their migration, transformation, bioavailability and toxicity in environmental mediums. Although the applied experimental conditions in this study are somewhat different from the real environmental conditions, the results herein may provide an important theoretical principle for predicting the change tendency of trace metals in real environmental mediums and further have a potential application in controlling heavy metal pollution.

This work was financially supported by the National Natural Science Foundation of China (20907055, 20971126 & 21077107), the National Basic Research Program of China (2011CB933700), the Knowledge Innovation Program of CAS and Special Foundation for High-level Waste Disposal (2007-840). The authors gratefully acknowledge Dr. Zhi Xie, Bo He and Fengchun Hu of NSRL, USTC for helpful technical assistance of EXAFS data collection and analysis.

1 Faur-Brasquet C, Kadirvelu K, Le Cloirec P. Removal of metal ions from aqueous solution by adsorption onto activated carbon cloths: Adsorption competition with organic matter. *Carbon*, 2002, 40: 2387–2392
2 Gonzalez-Serrano E, Cordero T, Rodriguez-Mirasol J, Cotoruelo L, Rodriguez JJ. Removal of water pollutants with activated carbons prepared from H_3PO_4 activation of lignin from kraft black liquors. *Water Res*, 2004, 38: 3043–3050
3 Hale SE, Tomaszewski JE, Luthy RG, Werner D. Sorption of dichlorodiphenyltrichloroethane (DDT) and its metabolites by activated carbon in clean water and sediment slurries. *Water Res*, 2009, 43: 4336–4346
4 Osmanlioglu AE. Treatment of radioactive liquid waste by sorption on natural zeolite in Turkey. *J Hazard Mater*, 2006, 137: 332–335
5 Rao GPC, Satyaveni S, Ramesh A, Seshaiah K, Murthy KSN, Choudary NV. Sorption of cadmium and zinc from aqueous solutions by zeolite 4A, zeolite 13X and bentonite. *J Environ Manage*, 2006, 81: 265–272
6 Ochoa-Herrera V, Sierra-Alvarez R. Removal of perfluorinated surfactants by sorption onto granular activated carbon, zeolite and sludge. *Chemosphere*, 2008, 72: 1588–1593
7 Yang ST, Sheng GD, Tan XL, Hu J, Du JZ, Montavon G, Wang XK. Determination of Ni(II) uptake mechanisms on mordenite surfaces: a combined macroscopic and microscopic approach. *Geochim Cosmochim Acta*, 2011, 75: 6520–6534
8 Hu J, Xie Z, He B, Sheng G, Chen C, Li J, Chen Y, Wang X. Sorption of Eu(III) on GMZ bentonite in the absence/presence of humic acid studied by batch and XAFS techniques. *Sci China Chem*, 2010, 53: 1420–1428
9 Schmidt GT, Vlasova N, Zuzaan D, Kersten M, Daus B. Adsorption mechanism of arsenate by zirconyl-functionalized activated carbon. *J Colloid Interface Sci*, 2008, 317: 228–234
10 Ankudinov AL, Rehr JJ. Relativistic calculations of spin-dependent X-ray absorption spectra. *Phys Rev B*, 1997, 56: 1712–1715
11 Strawn, DG, Scheidegger, AM, Sparks, DL. Kinetics and mechanisms of Pb(II) sorption and desorption at the aluminum oxide-water interface. *Environ Sci Technol*, 1998, 32: 2596–2601
12 Sheng GD, Yang ST, Sheng J, Hu J, Tan XL, Wang XK. Macroscopic and microscopic investigation of Ni(II) sequestration on diatomite by batch, XPS and EXAFS techniques. *Environ Sci Technol*, 2011, 45: 7718–7726
13 Scheidegger, AM, Strawn, DG, Lamble, GM, Sparks, DL. The kinetics of mixed Ni-Al hydroxide formation on clay and aluminum oxide minerals: A time-resolved XAFS study. *Geochim Cosmochim Acta*, 1998, 62: 2233–2245
14 Thompson, HA, Parks, GA, Brown, GE Jr. Dynamic interactions of dissolution, surface adsorption, and precipitation in an aging cobalt(II)-clay-water system. *Geochim Cosmochim Acta*, 1999, 63: 1767–1779
15 Shao D, Xu D, Wang S, Fan Q, Wu W, Dong Y, Wang X. Modeling of radionickel sorption on MX-80 bentonite as a function of pH and ionic strength. *Sci China Ser B-Chem*, 2009, 52: 362–371
16 Yang ST, Li JX, Shao DD, Hu J, Wang XK. Adsorption of Ni(II) on oxidized multi-walled carbon nanotubes: effect of contact time, pH, foreign ions and PAA. *J Hazard Mater*, 2009, 166: 109–116
17 Wuhan University. *Analytical Chemistry* (5th ed). Beijing: Higher Education Press, 2006, 385–403
18 Reddad Z, Gerente C, Andres Y, Le Cloirec P. Adsorption of several metal ions onto a low-cost biosorbent: kinetic and equilibrium studies. *Environ Sci Technol*, 2002, 36: 2067–2073
19 Chen CL, Wang XK. Adsorption of Ni(II) from aqueous solution using oxidized multiwall carbon nanotubes. *Ind Eng Chem Res*, 2006, 45: 9144–9149
20 Mercer KL, Tobiason JE. Removal of arsenic from high ionic strength solutions: Effects of ionic strength, pH, and preformed versus in situ formed HFO. *Environ Sci Technol*, 2008, 42: 3797–3802
21 Wang XS, Huang J, Hu HQ, Wang J, Qin Y. Determination of kinetic and equilibrium parameters of the batch adsorption of Ni(II) from aqueous solutions by Na-mordenite. *J Hazard Mater*, 2007, 142: 468–476
22 Huang JH, Liu YF, Wang XG. Selective adsorption of tannin from flavonoids by organically modified attapulgite clay. *J Hazard Mater*, 2008, 160: 382–387
23 Bhattacharyya KG, Gupta SS. Adsorption of Fe(III), Co(II) and Ni(II) on ZrO-kaolinite and ZrO-montmorillonite surfaces in aqueous medium. *Colloids Surf A*, 2008, 317: 71–79
24 Sheng GD, Yang ST, Zhao DL, Sheng J, Wang XK. Adsorption of Eu(III) on titanate nanotubes studied by a combination of batch and EXAFS technique. *Sci China Chem*, 2011, 54: 1–13
25 Collins CR, Vala RK, Sherman DM. Effect of inorganic and organic ligands on the mechanism of cadmium sorption to goethite. *Geochim Cosmochim Acta*, 1999, 63: 2989–3002
26 Buerge-Weirich B, Hari R, Xue H. Adsorption of Cu, Cd, and Ni on goethite in the presence of natural groundwater ligands. *Environ Sci Technol*, 2002, 36: 328–336
27 Boily JF, Sjoberg S, Persson P, Structures and stabilities of Cd(II) and Cd (II)-phthalate complexes at the goethite/water interface. *Geochim Cosmochim Acta*, 2005, 69: 3219–3235
28 Esmadi F, Simm J. Sorption of cobalt(II) by amorphous ferric hydroxide. *Colloids Surf A*, 1995, 104: 265–270
29 Tan XL, Wang XK, Chen CL, Sun AH. Effect of soil humic and fulvic acids, pH and ionic strength on Th(IV) sorption to TiO_2 nanoparticles. *Appl Radiat Isot*, 2007, 65: 375–381
30 Harter RD, Naidu R. An assessment of environmental and solution parameter impact on trace-metal sorption by soil. *Soil Sci Soc Am J*, 2001, 65: 597–612
31 Yang ST, Li JX, Lu Y, Chen YX, Wang XK. Sorption of Ni(II) on GMZ bentonite: effects of pH, ionic strength, foreign ions, humic acid and temperature. *Appl Radiat Isot*, 2009, 67: 1600–1608
32 Xu D, Tan XL, Chen CL, Wang XK. Removal of Pb(II) from aqueous solution by oxidized multiwalled carbon nanotubes. *J Hazard Mater*, 2008, 154: 407–416
33 Fan QH, Shao DD, Lu Y, Wu WS, Wang XK. Effect of pH, ionic strength, temperature and humic substances on the sorption of Ni(II) to Na-attapulgite. *Chem Eng J*, 2009, 150: 188–195
34 Shukla A, Zhang YH, Dubey P, Margrave JL, Shukla SS. The role of sawdust in the removal of unwanted materials from water. *J Hazard Mater*, 2002, 95: 137–152

35 Tan XL, Hu J, Montavon G, Wang XK. Sorption speciation of nickel(II) onto Ca-montmorillonite: batch, EXAFS techniques and modeling. *Dalton Trans*, 2011, 40: 10953–10960
36 Bargar JR, Brown GE Jr, Parks GA. Surface complexation of Pb(II) at oxide-water interfaces: I. XAFS and bond-valence determination of mononuclear and polynuclear Pb(II) sorption products on aluminum oxides. *Geochim Cosmochim Acta*, 1997, 61: 2617–2637
37 Cheah SF, Brown, GE Jr, Parks GA. XAFS spectroscopy study of Cu(II) sorption on amorphous SiO_2 and γ-Al_2O_3: Effect of substrate and time on sorption complexes. *J Colloid Interface Sci*, 1998, 208: 110–128
38 Dähn R, Scheidegger AM, Manceau A, Schlegel ML, Baeyens B, Bradbury MH, Morales M. Neoformation of Ni phyllosilicate upon Ni uptake on montmorillonite: a kinetics study by powder and polarized extended X-ray absorption fine structure spectroscopy. *Geochim Cosmochim Acta*, 2002, 66: 2335–2347
39 Dähn R, Scheidegger AM, Manceau A, Schlegel ML, Baeyens B, Bradbury MH, Chateigner D. Structural evidence for the sorption of Ni(II) atoms on the edges of montmorillonite clay minerals: a polarized X-ray absorption fine structure study. *Geochim Cosmochim Acta*, 2003, 67: 1–15
40 Lee S, Anderson PR, Bunker GB, Karanfil C. EXAFS study of Zn sorption mechanisms on montmorillonite. *Environ Sci Technol*, 2004, 38: 5426–5432
41 Scheidegger AM, Strawn DG, Lamble GM, Sparks DL. The kinetics of mixed Ni-Al hydroxide formation on clay and aluminum oxide minerals: a time-resolved XAFS study. *Geochim Cosmochim Acta*, 1998, 62: 2233–2245
42 Mandaliev P, Dähn R, Tits J, Wehrli B, Wieland E. EXAFS study of Nd(III) uptake by amorphous calcium silicate hydrates (C-S-H). *J Colloid Interface Sci*, 2010, 342: 1–7
43 Charlet L, Manceau A. Evidence for the neoformation of clays upon sorption of Co(II) and Ni(II) on silicates. *Geochim Cosmochim Acta*, 1994, 58: 2577–2582
44 Spadini L, Manceau A, Schindler PW, Charlet L. Structure and stability of Cd^{2+} surface complexes on ferric oxides. I. results from EXAFS spectroscopy. *J Colloid Interface Sci*, 1994, 168: 73–86
45 Roberts DR, Scheidegger AM, Sparks DL. Kinetics of mixed Ni-Al precipitate formation on a soil clay fraction. *Environ Sci Technol*, 1999, 33: 3749–3754
46 Ford RG, Scheckel KG, Sparks DL, Scheinost AC. The link between clay mineral weathering and the stabilization of Ni surface precipitates. *Environ Sci Technol*, 1999, 33: 3140–3144
47 Elzinga EJ, Sparks DL. Reaction condition effects on nickel sorption mechanisms in illite-water suspensions. *Soil Sci Soc Am J*, 2001, 65: 94–101
48 Strathmann TJ, Myneni SB. Effect of soil fulvic acid on nickel(II) sorption and bonding at the aqueous-boehmite (γ-AlOOH) interface. *Environ Sci Technol*, 2005, 39: 4027–4034
49 Papelis C, Brown GE Jr, Parks GA, Leckie JO. X-ray-absorption spectroscopic studies of cadmium and selenite adsorption on aluminum-oxides. *Langmuir*, 1995, 11: 2041–2048